Low-Temperature Fluorescence from Single Chlorosomes, Photosynthetic Antenna Complexes of Green Filamentous and Sulfur Bacteria

Yutaka Shibata,* Yoshitaka Saga,† Hitoshi Tamiaki,† and Shigeru Itoh*

*Department of Physics, Graduate School of Science, Nagoya University, Nagoya 464-8602, Japan; and †Department of Bioscience and Biotechnology, Faculty of Science and Engineering, Ritsumeikan University, Kusatsu, Shiga, Japan

ABSTRACT Fluorescence spectra of single chlorosomes isolated from a green filamentous bacterium (*Chloroflexus* (*Cfl.*) *aurantiacus*) and a green sulfur bacterium (*Chlorobium* (*Cb.*) *tepidum*) were measured by using a confocal laser microscope at 13 K. Chlorosomes were frozen either in a liquid solution (floating chlorosome) or on a quartz plate after being adsorbed (adsorbed chlorosome). Fluorescence peak wavelengths were shorter for the adsorbed single chlorosomes than for the floating ones. Single floating *Cfl.* chlorosomes showed a distribution of fluorescence peak positions having a center at 759.0 nm with a full width at half maximum of 6.3 nm. Single floating *Cb.* chlorosomes showed a 782.7 nm center with a full width at half-maximum of 3.4 nm. The distribution shifted to the blue and became wider with increasing temperature, especially in *Cb.* chlorosomes, suggesting a large excitonic density of states just above the lowest level. Energy transfer from BChl-*c* aggregates to BChl-*a* molecules in the baseplate proteins was observed in the floating chlorosomes but not in the adsorbed ones. A positive correlation was found between the peak wavelength of BChl-*c* fluorescence and the intensity of BChl-*a* fluorescence in single *Cfl.* chlorosomes. The results suggest that the BChl-*c* aggregates with longer wavelengths of the fluorescence peaks have a more efficient Förster-type energy transfer to the baseplate BChl-*a*.

INTRODUCTION

Photosynthetic green sulfur and filamentous bacteria contain chlorosomes that are attached to the membrane surface and transfer the absorbed solar energy to the reaction center complex (1,2). Chlorosomes contain a unique self-aggregated architecture of bacteriochlorophyll (BChl) molecules that are surrounded by a monolayer of lipids (3–8). The supramolecular structure is completely different from those of other antenna complexes that contain pigments inside proteins as protein-pigment complexes. Chlorosomes contain the aggregates of a huge number of BChl-*c*, -*d*, or -*e* molecules and small amounts of BChl-*a*, carotenoids, quinones (9,10), and proteins, although their locations inside chlorosomes are not yet clearly understood. The pigment aggregates designated $(\text{BChl-}c)_n$ in this study are assumed to be located at the chlorosomal core surrounded by a lipid monolayer and to funnel light energy into the BChl-*a* in baseplate proteins embedded in the monolayer. The energy is then transferred to the FMO protein and to the type I reaction center complex in the cytoplasmic bilayer membrane in green sulfur bacteria such as *Chlorobium* (*Cb.*) *tepidum*. In cells of the green filamentous bacterium *Chloroflexus* (*Cfl.*) *aurantiacus*, the baseplate BChl-*a* transfers energy to the core antenna BChl-*a* protein in the bilayer membrane and then to the type II reaction center. The chlorobium quinone contained in the chlorosomes of *Cb.* species seems to quench the excess excitation energy from $(\text{BChl-}c)_n$ under oxidative conditions (7). The efficient energy transfer (ET) inside chlorosomes seems to be also enabled by a sufficient overlap of the Q_y absorption bands of baseplate BChl-*a* molecules with the fluorescence bands of $(\text{BChl-}c)_n$ in both *Cb.* and *Cfl.* chlorosomes.

The self-aggregates of BChl-*c* have been assumed to form rodlike structures with diameters of 5–10 nm and lengths of 100–200 nm based on electron microscope images of freeze-fractured bacterial cells (3,4). The rod diameters are larger in *Cb.* chlorosomes than in *Cfl.* Several models have been proposed for the molecular architecture of the BChl-*c* self-aggregates to interpret the physicochemical properties of chlorosomes (5,8,11–16). One of the models (rod-type parallel packing) interprets well the result obtained by nuclear magnetic resonance (NMR) (17–20). Theoretical calculations assuming the exciton couplings among densely packed pigments in this model have also explained various spectroscopic results, such as the broad absorption spectrum shifted to the longer wavelength, linear dichroism, and circular dichroism spectra (13,21). However, the supramolecular structure of the pigment aggregates in chlorosome is still under debate. Pšenčík et al. (14) recently proposed a new model that assumes stacks of lamellar-like sheets for BChl-*c* aggregates based on their x-ray scattering experiment. This model is incompatible with the rod models. New types of experimental approaches are required to understand the relation between efficient energy transfer and pigment organization in chlorosomes.

Submitted March 27, 2006, and accepted for publication August 9, 2006.

Address reprint requests to Yutaka Shibata, Dept. of Physics, Graduate School of Science, Nagoya University, Nagoya 464-8602, Japan. Fax: 81-52-789-2883; E-mail: yshibata@bio.phys.nagoya-u.ac.jp.

Yoshitaka Saga's present address is Dept. of Chemistry, Faculty of Science and Engineering, Kinki University, Higashi-Osaka 577-8502, Japan.

0006-3495/06/11/3787/10 $2.00

doi: 10.1529/biophysj.106.084178

We have measured the fluorescence spectra of single chlorosomes of *Cfl. aurantiacus* and *Cb. tepidum* at room temperature (22–24) and at 12 K (25). The results have provided new information about the architecture of chlorosomes (25). In ordinary spectroscopy, averaging over the spectra of numerous molecules usually obscures the fine structures retained in the spectrum of a single molecule. The expected sharp responses of single molecules to the polarization of the excitation/detection light beams give valuable information on the electronic states of pigments (26), as indicated clearly in the study of the excitation spectra of a single peripheral antenna complex, LH2, of purple bacteria (27). The study provided crucial information on the structure of excited states responsible for the B800 and B850 absorption bands. In this study, we measured the fluorescence of single chlorosomes at 13 K to clarify the excited-state properties of (BChl-*c*)$_n$ in chlorosomes.

Chlorosomes of *Cfl. aurantiacus* and *Cb. tepidum* differ in size, structure, and spectroscopic properties. The sizes vary over a wide range, with average dimensions of 100 × 32 × 12 nm for *Cfl.* chlorosomes and 140 × 45 × 18 nm for *Cb.* chlorosomes (28). It has been estimated that the rods have a diameter of ~5 nm in *Cfl.* chlorosomes but a larger diameter of ~10 nm in *Cb.* chlorosomes (3,4). Results of an NMR study by van Rossum et al. (20) suggested that the rods are made of one and two layers of BChl-*c* self-aggregated sheet(s) in *Cfl.* and *Cb.* chlorosomes, respectively. Purified *Cfl.* chlorosomes show a Q_y absorption peak of (BChl-*c*)$_n$ at 741 nm, with a fluorescence peak at 750 nm at room temperature. The fluorescence peak of BChl-*a* in the baseplate is around 803 nm. Purified *Cb.* chlorosomes show a Q_y absorption peak of (BChl-*c*)$_n$ at 742 nm, with a fluorescence peak at 766 nm and fluorescence from BChl-*a* in the baseplate as a shoulder around 810 nm. The different optical properties of chlorosomes between two organisms seem to reflect the different structures of pigment aggregates, although the relation is not yet clear.

In this article, we report the results of fluorescence spectroscopy of single chlorosomes. The results provide information related to the optical properties of chlorosomes and the model calculations of the exciton state formulated based on the fine molecular models. Although the fluorescence of single chlorosomes adsorbed to quartz surfaces did not show an ET from (BChl-*c*)$_n$ to BChl-*a* in the baseplate (22,23), single chlorosomes that were frozen in the reaction medium revealed strong fluorescence from BChl-*a* in the baseplate upon the indirect excitation of (BChl-*c*)$_n$ (25). In this study, we examined the ET process inside single chlorosomes of *Cfl. aurantiacus* and *Cb. tepidum* at 13 K.

MATERIALS AND METHODS

Preparation of two types of single chlorosomes

Chlorosomes from *Cfl. aurantiacus* Ok-70-fl and *Cb. tepidum* ATCC49652 were purified according to the method described previously (29). The purified chlorosomes were suspended in a medium containing 50 mM Tris-HCl (pH 8.0). Sodium dithionite was added to the medium to reduce oxidative components in chlorosomes at a final concentration of 10 mM. Two types of samples were prepared as follows. 1), ''Floating chlorosomes,'' chlorosomes suspended in the above-mentioned medium containing 50% glycerol (v/v) were sealed in a cavity between two quartz windows kept 50 μm apart from each other with a Teflon spacer to give 0.03 OD/cm at a Q_y peak of (BChl-*c*)$_n$, as described previously (25). 2), ''Chlorosomes adsorbed on a quartz plate'' were prepared by pouring the medium containing the chlorosome onto a quartz plate and then washing out the unbound chlorosome, as described previously (22,23). The above-mentioned medium/glycerol mixture containing 10 mM sodium dithionite was then poured onto the chlorosome-adsorbed quartz plate and was sealed with another quartz plate and a Teflon spacer. The two types of chlorosome samples were placed in a homemade copper sample holder, set in a liquid-He-flow-type cryostat (Microstat, Oxford Instruments, Eynsham, UK), and measured at 13 ± 0.5 K with a temperature controller (ITC4, Oxford Instruments). The measurement at 13 K immobilized chlorosomes in frozen solvents and suppressed irradiation damage from the strong excitation laser beam. Sodium dithionite was added to samples just before sealing. Samples were cooled after incubation for ~30 min at room temperature. This procedure might not have been sufficient for a complete reduction of samples, especially in the case of *Cb.* chlorosome, and might have resulted in the low efficiency of energy transfer from (BChl-*c*)$_n$ to BChl-*a* (see Results). We did not apply a longer incubation period because it could have resulted in reoxidation by air oxygen molecules due to the small sample volume and the rather large surface area. For *Cfl.* chlorosome, which is less sensitive to the reducing condition, this procedure seems sufficient to enable efficient energy transfer (see Results).

Fluorescence spectroscopy of single chlorosomes

Fluorescence from single chlorosomes was measured by a laser-scanning confocal microscope system (Nanofinder, Tokyo-Instruments, Tokyo, Japan) equipped with a 52-cm monochromator. The fluorescence of each chlorosome was excited with a focused 458-nm excitation beam of an Ar^+ ion laser (5490ASL-00, Nippon Laser, Tokyo) at a Soret peak of (BChl-*c*)$_n$. The excitation beam slightly excited BChl-*a* in the baseplate protein with a Soret peak at ~380 nm. The laser beam was focused on each chlorosome in the cryostat by using a ×40 objective lens (Plan Fluor 40×, Nikon, Tokyo, Japan, with N/A of 0.6, working distance of 3.7 mm) of the microscope (TE300, Nikon). Each fluorescence image at a different *z*-position was obtained by *x*-*y* scanning of the focusing point with a galvanic mirror and by *z* scanning with a piezometer system. Collection and excitation of fluorescence were done with the same objective lens. The fluorescence was passed through a dichroic mirror, a notch filter, and a long-pass filter to reject laser scattering, and then was focused onto the entrance slit of the monochromator, which has vertical and horizontal slits to adjust the spatial and wavelength resolutions. The widths of the entrance slits were set at 80 μm to give spatial resolutions of 1 μm for both the *x* and *y* axes and 5 μm for the *z* axis.

Fluorescence was detected either by a cooled photon-counting photomultiplier (R943-02, Hamamatsu photonics, Hamamatsu, Japan) to scan images or by a cooled CCD detector (DU420-BV, Andor Technology, Belfast, UK) to obtain spectra. In this study, sensitivity correction was not applied to the observed fluorescence spectra. We confirmed that sensitivity correction induces only a small deformation of spectra because of the very sharp spectral width of single chlorosomes at cryogenic temperatures. The intensity of the excitation laser beam was set at 2–8 μW at the focusing point. The intensity corresponds to 1–4 × 10^3 W/cm^2 and is two to three orders of magnitude higher than that of solar energy. As described in the text, fluorescence intensities of single chlorosomes were rather stable during the measurement under this excitation intensity at 10–20 K.

RESULTS

Detection of single ''floating'' and ''adsorbed'' chlorosomes

Fig. 1, *A* and *C*, shows fluorescence images of ''floating chlorosomes'' prepared from *Cb. tepidum* that were dispersed in a water-glycerol mixture and frozen to 13 K in a cryostat. The *x-y* images were obtained at each depth of the *z* axis at 4-μm intervals. Each bright spot in the image corresponds to the fluorescence from a single chlorosome. The ''floating chlorosomes'' showed bright spots at different positions in the *x-y* images at different *z*-positions, showing their three-dimensional distribution. Fluorescence from chlorosomes outside the focal plane gave sparse spots with lower intensities. Fig. 1 *D* shows the fluorescence image of ''adsorbed chlorosomes'' from *Cb. tepidum*, which were fixed on a quartz plate at room temperature, as previously described (22), and measured at 13 K. The image showed bright spots only at one z-depth, as expected.

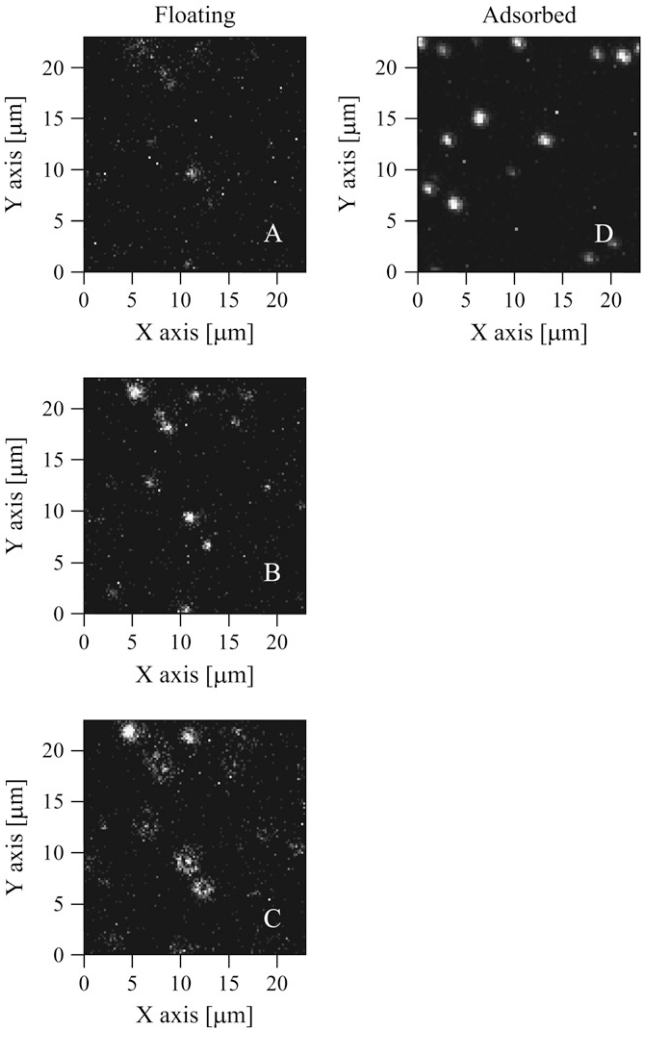

FIGURE 1 Typical fluorescence images of the floating chlorosomes (*left side*) at different *z* axis positions at intervals of 4 μm (*A–C*) and adsorbed chlorosomes (*D, right side*) isolated from *Cb. tepidum* at 13 K. The white spots represent the sites of high fluorescence intensity.

Fluorescence spectra of single chlorosomes of *Cfl. aurantiacus*

Solid lines in Fig. 2 show the fluorescence spectra of single ''floating chlorosomes'' normalized at their peak intensities (*A*) and ''adsorbed chlorosomes'' (*B*) of *Cfl. aurantiacus* at 13 K. These spectra were obtained by focusing the laser on each spot in the prescanned image. Each spectrum typically was obtained by accumulating 10 successive measurements for 1 s. No appreciable change was detected in the spectral shape or intensities during the accumulation. The two peaks at 750–765 nm and 810–825 nm can be attributed to the fluorescence from (BChl-*c*)$_n$ and from BChl-*a* in the baseplate protein, respectively. The intensities of the BChl-*a* peaks in the normalized spectra give measures for the

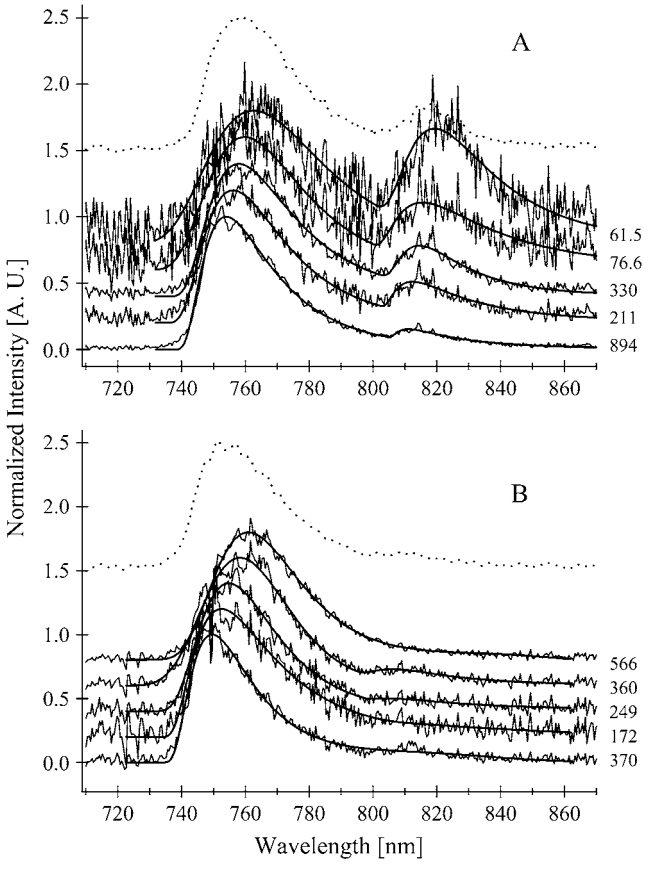

FIGURE 2 Fluorescence spectra of floating (*A*) and adsorbed (*B*) single chlorosomes purified from *Cfl. aurantiacus*. Spectra are offset vertically to avoid overlap. The smooth lines are the fitting curves calculated as the sum of skewed Gaussian functions as described in text. Numbers on the right of the spectra are normalization factors. Dotted line is the sum of the spectra of 125 floating chlorosomes or 94 adsorbed chlorosomes. Each spectrum is normalized at the (BChl-*c*)$_n$ peaks around 760 nm.

efficiencies of ET from (BChl-c)$_n$ to BChl-a, because the laser at 458 nm excites (BChl-c)$_n$ almost exclusively. Floating chlorosomes with the stronger BChl-a band gave fluorescence peaks at wavelengths somewhat longer than those of adsorbed chlorosomes. The results seem to come from either the lower ET efficiency to BChl-a or the stronger quenching of BChl-a fluorescence in the adsorbed chlorosomes. Single chlorosomes with the longer peak wavelengths of (BChl-c)$_n$ seem to give stronger BChl-a fluorescence. The dotted lines in Fig. 2 show the averaged spectra for >100 single chlorosomes. The spectra thus approximate the ensemble spectra that can be obtained as the sum of all the spectra and corresponds to the spectrum of the whole solution measured by ordinary fluorometry. The bandwidths of the averaged spectra were a little broader than that of a single chlorosome spectrum, indicating the broad fluorescence profiles of single chlorosomes.

For further analysis, we fitted the obtained spectra as the sum of two skewed Gaussian curves expressed as (30,31)

$$F(\nu) = \sum_{i=1}^{2} F_i \exp\left(-\ln 2 \cdot \left[\frac{\ln(1 + 2b_i(\nu - \nu_{max,i})/\Delta\nu_i)}{b_i}\right]^2\right). \quad (1)$$

Here, F_i, $\nu_{max,i}$, and $\Delta\nu_i$ are the height, peak wave number, and bandwidth, respectively, of the ith component. b_i is the asymmetry parameter. When b is negative/positive, the curve shows a gentler slope on the side of the lower/higher wavenumber. At the limit of $b_i = 0$, the curve converges to a symmetric Gaussian. We assigned the first and second components to (BChl-c)$_n$ and BChl-a fluorescence bands, respectively. F_1 and F_2, then, represent their peak heights, denoted as $F_{BChl\text{-}c}$ and $F_{BChl\text{-}a}$, respectively. We applied the skewed Gaussian shape to simulate an asymmetric spectrum observed in this experiment.

The smooth solid lines in Fig. 2 are fitting curves obtained by using Eq. 1. The spectra are expressed as functions of wavelength, although the fitting was done based on wave number. Hereafter, $\lambda_{BChl\text{-}c}$ and $\lambda_{BChl\text{-}a}$ denote inverses of $\nu_{max,1}$ and $\nu_{max,2}$, respectively. The experimental data were well fitted by model curves calculated with two skewed Gaussian components according to Eq. 1, with eight parameters in the iteration program.

We obtained the statistical properties by fitting the fluorescence spectra of 125 floating and 94 adsorbed *Cfl.* chlorosomes. In both cases, the set of spectra of single chlorosomes, which were obtained for the same sample in the two independent measurements on different days, gave consistent results, confirming the high reliability of the results of this experiment and analysis. We analyzed the chlorosome samples that were prepared on one day to minimize deviations due to differences in growth conditions, stages, and other factors, which could induce additional inhomogeneities. Intact and baseplate-depleted chlorosomes showed similar fluorescence spectral properties of single chlorosomes, indicating the reproducibility of this experimental procedure (24).

Fig. 3 shows the histogram of $\lambda_{BChl\text{-}c}$ for floating and adsorbed *Cfl.* chlorosomes. The $\lambda_{BChl\text{-}c}$ values gave a narrow distribution in each case. The peaks of distributions were estimated by fitting to symmetrical Gaussian curves (*dotted lines*) at 759.0 ± 0.4 nm and 755.0 ± 0.2 nm for floating and adsorbed chlorosomes, respectively, with almost equal full width at half maximum values of 6.3 ± 0.9 nm and 5.6 ± 0.5 nm, respectively. The peak for the floating chlorosomes was almost the same as that of the fluorescence spectrum of chlorosome solution. On the other hand, the peak for the adsorbed chlorosomes shifted by 4 nm to the blue, suggesting some modifications. A similar blue shift of the chlorosome spectrum upon adsorption on a glass surface was also observed in the previous study at room temperature (23). The shift induced by the adsorption resembles that reported in bacteriorhodopsin adsorbed to a glass surface (32), although its mechanism is not yet clear.

Fig. 2 suggests that the *Cfl.* single chlorosomes with (BChl-c)$_n$ peaks at the longer wavelengths show the stronger fluorescence of BChl-a; in other words, they show the higher efficiency of ET to BChl-a. To confirm this possibility, we

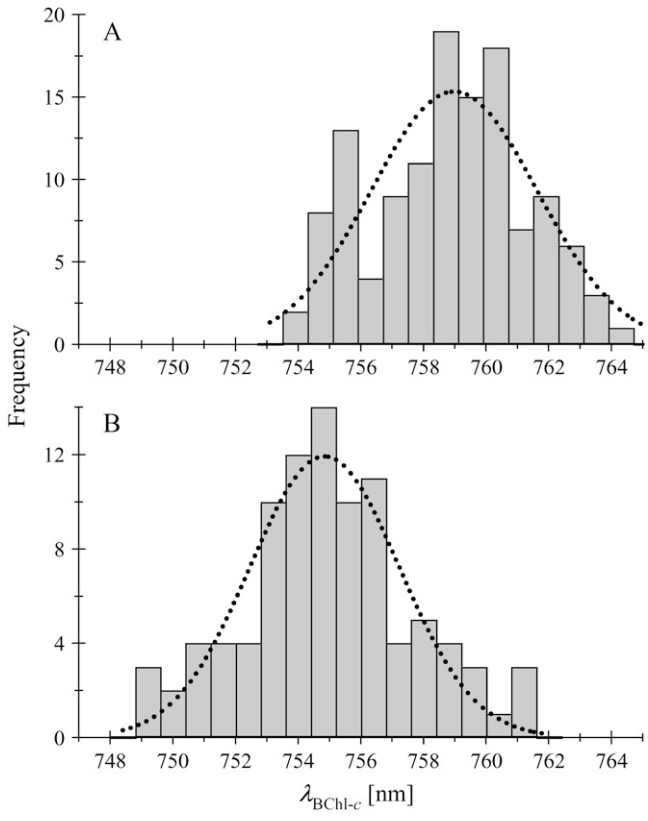

FIGURE 3 Distribution of the fluorescence peak wavelengths of single chlorosomes from *Cfl. aurantiacus*. Shaded sticks show the histogram of the $\lambda_{BChl\text{-}c}$ of the floating (*A*) and the adsorbed (*B*) single chlorosomes. Dotted lines are the fitting curves to Gaussian functions.

calculated the ratio of fluorescence intensity $F_{\text{BChl-}a}/F_{\text{BChl-}c}$ in each chlorosome. The circles in panel *A* of Fig. 4 show the ratio plotted against $\lambda_{\text{BChl-}c}$ for floating chlorosomes. A positive correlation between $F_{\text{BChl-}a}/F_{\text{BChl-}c}$ and $\lambda_{\text{BChl-}c}$ was detected with a correlation coefficient of 0.44 despite a severe scattering of the data. For the adsorbed chlorosomes, on the other hand, the $F_{\text{BChl-}a}/F_{\text{BChl-}c}$ ratio was low and revealed almost no apparent correlation with $\lambda_{\text{BChl-}c}$ (data not shown).

The asymmetrical parameter *b* showed an obvious correlation with $\lambda_{\text{BChl-}c}$ in the floating chlorosomes as shown by triangles in Fig. 4 *B*. The smaller the $\lambda_{\text{BChl-}c}$ value, the higher the negative *b* value that represents the gentler slope on the longer wavelength side. Correlation coefficients between the *b* and $\lambda_{\text{BChl-}c}$ values of 0.74 and 0.67 were obtained for the floating and the adsorbed chlorosomes, respectively, indicating that the correlation is also the case for the adsorbed chlorosomes (data not shown). In Fig. 4 *C*, $\lambda_{\text{BChl-}a}$ is plotted *vs.* $\lambda_{\text{BChl-}c}$, and a correlation coefficient of 0.67 was obtained for the floating chlorosomes.

Fluorescence of single chlorosomes of *Cb. tepidum*

Fig. 5 shows the fluorescence spectra of floating (*A*) and adsorbed (*B*) single chlorosomes of *Cb. tepidum*. The fluorescence band widths of $(\text{BChl-}c)_n$ in *Cb.* chlorosomes are slightly narrower than those in *Cfl. aurantiacus* chlorosomes. Two types of fluorescence profiles are noted: one with a shoulder on the shorter-wavelength side and the other without a shoulder. The fluorescence from the baseplate BChl-*a* around 820 nm was hardly detected in the adsorbed chlorosomes and was very weak even in the floating ones. Thick solid lines are the fitting curves. Three skewed Gaussian curves are necessary to fit each spectrum sufficiently; the two components are required to fit the $(\text{BChl-}c)_n$ band, and the one component to fit the BChl-*a* band. $\lambda_{\text{BChl-}c}$

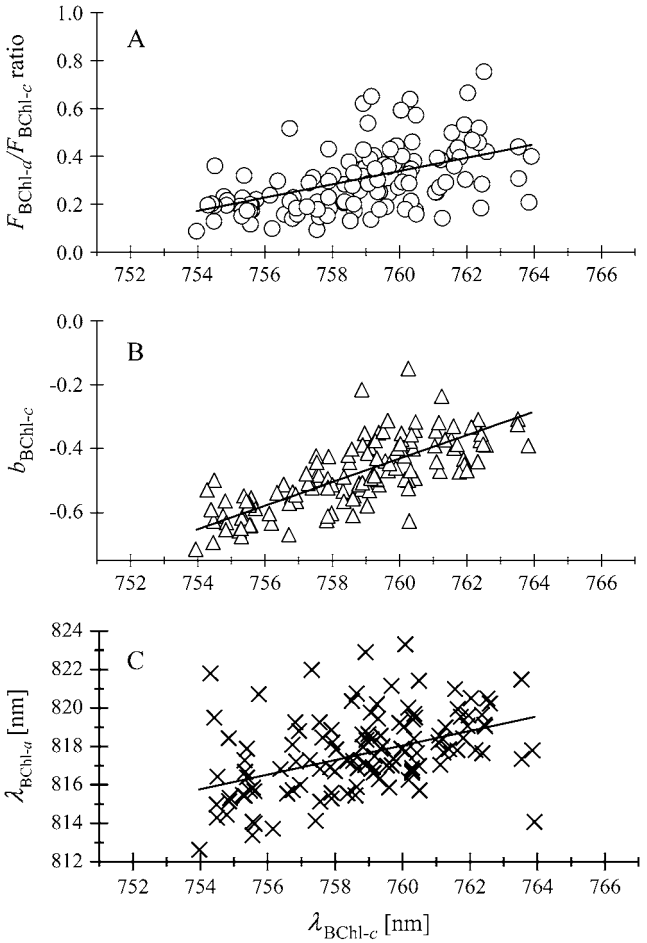

FIGURE 4 Plots of $F_{\text{BChl-}a}/F_{\text{BChl-}c}$ ratio (*A*, *open circles*), $b_{\text{BChl-}c}$ value (*B*, *open triangles*), and $\lambda_{\text{BChl-}a}$ value (*C*, *crosses*) against $\lambda_{\text{BChl-}c}$ for single chlorosomes from *Cfl. aurantiacus*. Solid lines represent fitting to linear curves.

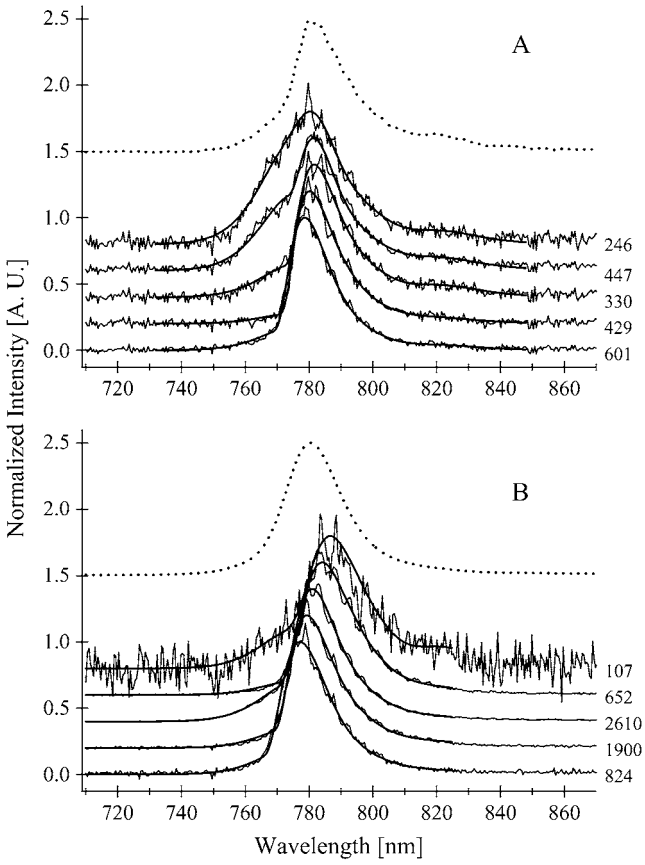

FIGURE 5 Fluorescence spectra of floating (*A*) and adsorbed (*B*) single chlorosomes purified from *Cb. tepidum*. Spectra are offset vertically to avoid overlap. The smooth lines represent the fitting curves to the sum of skewed Gaussian functions. Numbers on the right of the spectra are normalization factors. The dotted line is a sum of the spectra of 121 floating chlorosomes or 136 adsorbed chlorosomes. Each spectrum is normalized at the $(\text{BChl-}c)_n$ peaks around 780 nm.

and $F_{\mathrm{BChl}\text{-}c}$ hereafter represent the peak wavelength and the height of the major longer-wavelength component, respectively. The residual minor component was required to fit the short-wavelength shoulder of the $(\mathrm{BChl}\text{-}c)_n$ fluorescence band. Because of very weak fluorescence from BChl-*a*, ν_{max} of the BChl-*a* component was fixed to 12,132 cm^{-1} in the entire fitting procedure for *Cb*. chlorosomes.

Fitting was done for 121 floating and 136 adsorbed single *Cb*. chlorosomes. Histograms of $\lambda_{\mathrm{BChl}\text{-}c}$ are shown in Fig. 6. The peak of the distribution in the adsorbed chlorosomes (*B*) shifted to the blue compared to that in the floating ones (*A*), as in the case of *Cfl*. chlorosomes. The shift was smaller than that observed in *Cfl*. chlorosomes. We fitted the distribution profiles by Gaussian curves (*dotted lines*) at peak wavelengths of 782.7 ± 0.1 nm and 780.9 ± 0.1 nm with full width at half maximum values of 3.4 ± 0.3 nm and 3.9 ± 0.3 nm for the floating and the adsorbed chlorosomes, respectively.

Fig. 7 shows the correlations of $F_{\mathrm{BChl}\text{-}a}/F_{\mathrm{BChl}\text{-}c}$ versus $\lambda_{\mathrm{BChl}\text{-}c}$ (*A*), and the asymmetry parameter *b* versus $\lambda_{\mathrm{BChl}\text{-}c}$ (*B*) for the floating *Cb*. chlorosomes. Although the fluorescence from the baseplate BChl-*a* was very weak, $F_{\mathrm{BChl}\text{-}a}/F_{\mathrm{BChl}\text{-}c}$ and $\lambda_{\mathrm{BChl}\text{-}c}$ showed low correlation coefficients of 0.53 and 0.46 for the floating and the adsorbed chlorosomes, respectively (data not shown). The asymmetry parameter *b*, on the other hand, was around −0.64, regardless of the $\lambda_{\mathrm{BChl}\text{-}c}$ position. The detected ET efficiency was somewhat lower than that measured by ordinary fluorescence spectroscopy (33). The low efficiency might have resulted from the insufficient reduction of chlorosomes inside the cryostat cavity since the ET in *Cb*. chlorosomes is known to be extremely sensitive to the reducing conditions (2,9).

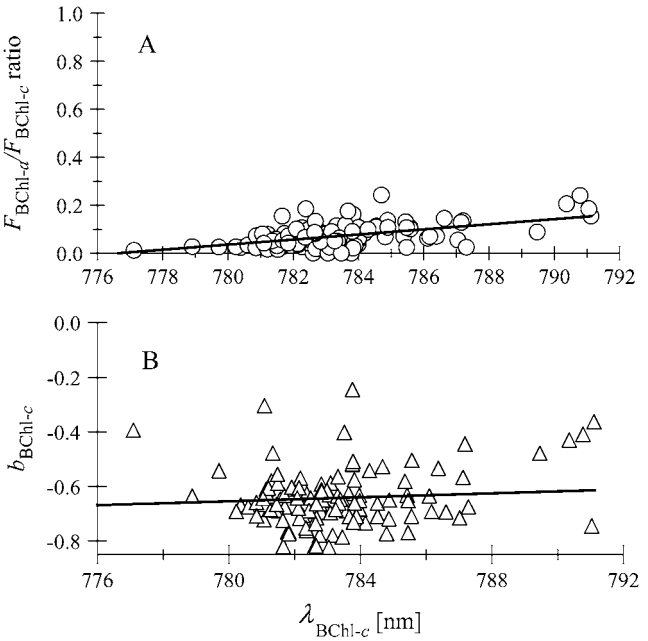

FIGURE 7 Plot of the $F_{\mathrm{BChl}\text{-}a}/F_{\mathrm{BChl}\text{-}c}$ ratio (*A*, *open circles*) and $b_{\mathrm{BChl}\text{-}c}$ value (*B*, *open triangles*) against the $\lambda_{\mathrm{BChl}\text{-}c}$ value for single chlorosomes from *Cb. tepidum*. Solid lines show fitting to linear curves.

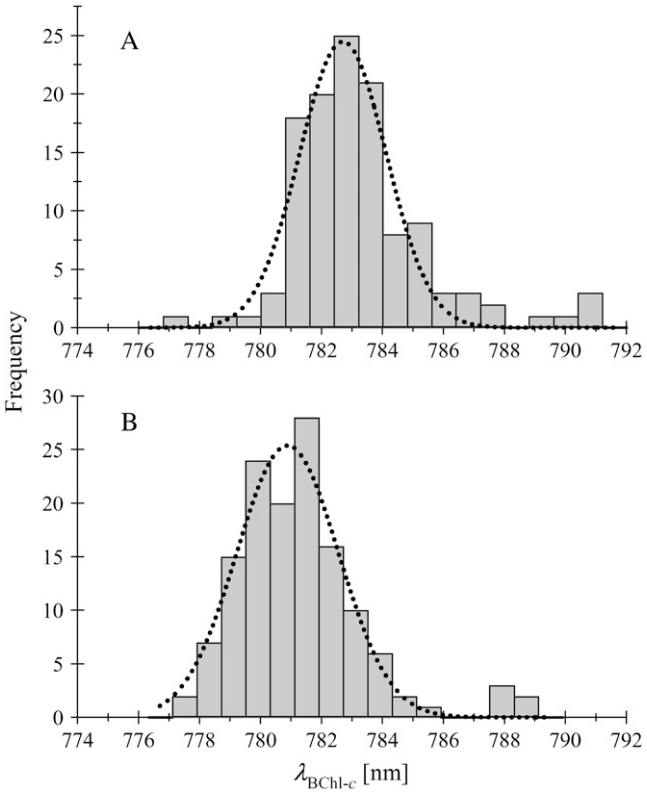

FIGURE 6 Distribution of the fluorescence peak wavelengths of single chlorosomes purified from *Cb. tepidum*. Shaded sticks show the histogram of the $\lambda_{\mathrm{BChl}\text{-}c}$ of the floating (*A*) and adsorbed (*B*) single chlorosomes. Dotted lines represent the fitting curves to Gaussian functions.

DISCUSSION

We measured the fluorescence spectra of $(\mathrm{BChl}\text{-}c)_n$ and baseplate BChl-*a* in single chlorosomes of *Cfl. aurantiacus* and *Cb. tepidum*. Each chlorosome showed different fluorescence spectrum. We observed the fluorescence of both ''floating'' single chlorosomes that were frozen in the medium and ''adsorbed'' single chlorosomes that were adsorbed to a quartz plate before freezing. Both the ''adsorbed'' and ''floating'' chlorosomes showed similar sizes and intensities of fluorescence spots in the scanning images, as shown in Fig. 1. The sizes of the spots were on the order of the spatial resolution of the experimental set-up described here, suggesting that they were emitted from single chlorosomes, as indicated by the previous AFM image of the adsorbed chlorosomes (22).

The physicochemical properties of chlorosomes studied here can be briefly summarized as follows. 1), Each single *Cfl*. or *Cb*. chlorosome showed a different spectral shape of fluorescence. 2), The adsorbed chlorosomes revealed fluorescence peaks at wavelengths 4–5 nm shorter than those

revealed by the floating chlorosomes. 3), (BChl-*c*)$_n$ in *Cfl.* single chlorosomes showed broader fluorescence spectra than *Cb.* single chlorosomes, which showed narrower bandwidths with a short-wavelength shoulder. 4), The peak wavelength $\lambda_{\text{BChl-}c}$ of fluorescence was distributed among single chlorosomes. The distribution was wider for *Cfl.* chlorosomes than for *Cb.* chlorosomes. The result is, however, opposite to the observation at room temperature for adsorbed chlorosomes (22, 23). 5), *Cfl.* chlorosomes showed efficient ET from (BChl-*c*)$_n$ to BChl-*a*. The ET efficiency was higher in the chlorosomes with the longer peak wavelengths of (BChl-*c*)$_n$ fluorescence.

Observation of fluorescence from single chlorosomes

The detection of fluorescence from a single molecule was facilitated by focusing the laser beam on the target. High laser intensity at the spot often damages the target sample. We used a ×40 objective lens with a numerical aperture of 0.6, which gave an excitation area of 1.8×10^{-8} cm^2 (1.8 μm^2) and high excitation power equivalent to 1–4 $\times 10^2$ W/cm^2 (1–4 μW/μm^2) on the spot. In this study, it was confirmed that the laser power did not induce severe degradations of pigments during the typical 10-s accumulation period of each fluorescence spectrum at 10–20 K. The time constant of the photodamage of chlorosomes at 13 K was >300 s (data not shown). On the other hand, based on the results of ordinary spectroscopy, Granzhan et al. (34) estimated the quantum yield ϕ_D of photodegradation of (BChl-*c*)$_n$ in chlorosomes of *Cb. tepidum* to be 8×10^{-7} at room temperature. Based on this ϕ_D value and an estimated absorption cross section of BChl-*c* at 458 nm of 3×10^{-16} cm^2, the laser power used in this study was expected to give a 4- to 17-s BChl-*c* degradation time constant, which was 20 times faster than the 13 K detected in this study. It is therefore concluded that the photodegradation rate decreases dramatically at cryogenic temperature and we can measure the fluorescence spectrum of an intact single chlorosome.

Fluorescence peaks of the single chlorosomes adsorbed to the quartz plate have been reported to shift to the shorter wavelength side at room temperature (22,23) or at 13 K (25), as shown in Figs. 2 and 5. Upon adsorption, *Cb.* chlorosomes showed larger blue shifts than did *Cfl.* chlorosomes. Adsorbed on a quartz surface, both the *Cfl.* and *Cb.* chlorosomes showed almost no fluorescence from the baseplate BChl-*a*. The adsorption to a glass surface thus alters the optical property and might modify the structure of chlorosomes. An atomic force microscope image obtained in the previous work (22) indicated that most of the chlorosomes were adsorbed on a quartz plate as a single complex along their long elliptical axes parallel to the surface. The baseplate proteins might have been preferentially adsorbed to a quartz surface in this orientation and thus been modified, as reported in the case of bacteriorhodopsin of *Halobacterium* adsorbed to a solid surface (32), although the mechanism for the blue shift has not yet been clarified.

By using an aligned *Cfl.* chlorosome sample in a squeezed polyacrylamide gel, Mimuro et al. (35) showed that the transition dipole moments of (BChl-*c*)$_n$ and the baseplate are, respectively, parallel and perpendicular to the long axis of a chlorosome. This observation might explain the low fluorescence intensity from the baseplate in the adsorbed chlorosomes because the orientations of the transition dipoles of the baseplate BChl-*a*, which is aligned almost parallel to the light path, may decrease the intensity of the detected fluorescence. The effect of orientation of chlorosomes on their fluorescence properties will be reported elsewhere.

The fluorescence intensity of BChl-*a* of *Cb.* chlorosomes was somewhat lower than that observed by ordinary fluorometry. This result might be due to insufficient reduction because the BChl-*a* fluorescence of *Cb.* chlorosomes is known to be much more sensitive to the reducing condition (2,9) than are *Cfl.* chlorosomes. Thus, we performed a quantitative analysis of energy transfer efficiency for *Cfl.* floating chlorosomes, as discussed in the following sections.

Fluorescence spectrum of single chlorosomes and the ensemble spectrum

The fluorescence spectrum, which can be measured by ordinary fluorometry in medium, should be realized as the ensemble of all the single-chlorosome spectra. For the ensemble of spectra, we calculated the average of the single-chlorosome spectra in this study. The ensemble spectra shown in Figs. 2 and 5 should, therefore, be equivalent to the bulk spectra. The fluorescence spectrum of intact cells of *Cfl.* at 10 K has been reported to peak at 759 nm (36), which is in good agreement with the averaged spectrum of the floating single chlorosomes (Fig. 2 *A*). For *Cb.* chlorosomes, the averaged fluorescence spectrum showed a peak at 782 nm (Fig. 5 *A*), which is in good agreement with the spectrum of the suspension of the purified chlorosome measured at the same temperature (33). Thus, the experimental condition described here seemed to induce no critical modification of floating chlorosomes, whereas the blue shift of the fluorescence spectra in the adsorbed chlorosomes indicates some alterations.

The fluorescence spectra of (BChl-*c*)$_n$ of single *Cfl.* chlorosomes were well fitted to a curve with one skewed Gaussian component. The spectra of single *Cb.* chlorosomes, on the other hand, showed a small short-wavelength shoulder band as shown in Fig. 5. The fitting of the spectra required an additional short-wavelength component to obtain sufficient agreement. The width of each component of the *Cb.* chlorosomes was appreciably sharper than that of the *Cfl.* single chlorosomes. Such a significant difference in the spectral profiles cannot be identified in the ensemble fluorescence spectra, which indicates different extents of disorder between the two types of chlorosomes.

Inhomogeneities in fluorescence spectra of single chlorosomes

The peak wavelength of fluorescence $\lambda_{\text{BChl-}c}$ at 13 K showed a wider distribution for *Cfl.* chlorosomes than for *Cb.* chlorosomes in both the adsorbed and floating chlorosomes. The result was, however, opposite to the case obtained previously with the adsorbed single chlorosomes at room temperature (22,23).

Here, we define two inhomogeneous distribution functions (IDFs) to distinguish the intra- and the inter-single-chlorosome inhomogeneities. We define the intra-IDF as the distribution of the lowest-energy levels of the emitting pigments (or excitonic states) in a single chlorosome. The inter-IDF, on the other hand, can be defined as the distribution of the peak position of the intra-IDF among single chlorosomes. To avoid confusion, hereafter we refer to the ordinary IDF as the overall IDF, represented by the convolution of the intra- and the inter-IDFs. The fluorescence profile of a single chlorosome, then, is roughly expressed by the convolution between the intra-IDF and the fluorescence profile of the lowest-emitting pigments or the excitonic state, that is, the homogeneous fluorescence profile (HFP). The width of the $\lambda_{\text{BChl-}c}$ distribution obtained in this study might be comparable to that of the inter-IDF, although the former is red-shifted from the latter. The red shift arises because the HFP does not show a δ-function shape at zero energy due to, for example, the phonon sideband on the long wavelength side.

The overall IDF of chlorosomes has been obtained by zero-phonon hole (ZPH) action spectroscopy (33,37), in which the depths of the sharp ZPHs are measured as a function of the burning wavelength with constant burning power and time. The overall IDF corresponds to the plot of the hole depth against the burning wavelength. Its width for the isolated chlorosome of *Cb. tepidum* has been reported as 11.3 nm (184 cm^{-1}) (33), which is more than three times larger than the width of the $\lambda_{\text{BChl-}c}$ distribution of 3.4 nm (55 cm^{-1}) in this study. The larger width of the overall IDF compared to that of the $\lambda_{\text{BChl-}c}$ distribution might be attributed to the additional contribution from the intra-IDF. If we assume Gaussian shapes for both the intra- and inter-IDFs, the width of the intra-IDF of *Cb.* chlorosomes is estimated to be 176 cm^{-1}, suggesting its dominant contribution to the overall IDF.

In the case of the chlorosomes of *Cfl. aurantiacus*, the overall IDF has been reported to have a width of 90 cm^{-1} (37), which is almost the same as or even smaller than the value of 6.3 nm (109 cm^{-1}) for the width of the $\lambda_{\text{BChl-}c}$ distribution of the floating *Cfl.* single chlorosomes. This result indicates that the width of the overall IDF is comparable to that of the inter-IDF, suggesting a minor contribution from the intra-IDF. The results of this study thus suggest a rather different extent of intra-inhomogeneity between *Cb.* and *Cfl.* chlorosomes. The small extent of the intra-inhomogeneity in *Cfl.* chlorosomes means that the broad fluorescence profiles of single *Cfl.* chlorosomes should be attributed mainly to the broadening of HFP rather than that of the intra-IDF. The much broader width of fluorescence profiles of single *Cfl.* chlorosomes compared to those of the overall IDF also corroborate a broad HFP. The phonon sideband might contribute to the broadening of the HFP, although further study is necessary to confirm this possibility.

In the previous article, the broad distribution of fluorescence peaks of *Cb.* single chlorosomes at room temperature has been ascribed to the existence of BChl-*c* homologs (23) that have different alkyl groups at the 8- and 12-positions. The homolog composition has also been reported to affect the spectroscopic properties of *Cb.* chlorosomes (38, 39). Thus, the substitution diversity has been considered to produce a broader $\lambda_{\text{BChl-}c}$ distribution for *Cb.* chlorosomes (23). On the other hand, *Cfl.* chlorosomes contain only one type of BChl-*c* with an ethyl group at the 8-position and a methyl group at the 12-position. The above consideration is consistent with the conclusion reached here, that the intra-IDF provides a major contribution to the broadening of the overall IDF in *Cb.* chlorosomes, whereas it has only a minor effect in *Cfl.* chlorosomes.

A comparison of the results of the previous study (23) with those in the present study can be summarized according to the order of widths of $\lambda_{\text{BChl-}c}$ distributions as follows: at room temperature, *Cb.* chlorosomes $>$ *Cfl.* chlorosomes; at 13 K, *Cb.* chlorosomes $<$ *Cfl.* chlorosomes. The inversion on cooling was due to a drastic narrowing of the distribution for *Cb.* chlorosomes. The distribution width for *Cfl.* chlorosomes was, on the other hand, almost temperature-independent. The $\lambda_{\text{BChl-}c}$ distribution at room temperature cannot be directly related to the inter-IDF because the fluorescence at room temperature is emitted not only from the lowest levels. We thus attribute the opposite relations of the widths of the $\lambda_{\text{BChl-}c}$ distribution at low and room temperatures to the difference in the excitonic densities of states between chlorosomes from two organisms. In *Cb.* chlorosomes, the fluorescence spectrum shows a larger blue shift upon warming due to the large excitonic density of states just above the lowest level, which might also promote the diversity in fluorescence peak wavelength at higher temperatures.

Correlation among various quantities

The single chlorosome measurements in this study gave correlations between various quantities, such as the positive correlation between the $F_{\text{BChl-}a}/F_{\text{BChl-}c}$ ratio and $\lambda_{\text{BChl-}c}$. The correlation was observed for both *Cfl.* and *Cb.* floating chlorosomes, with correlation coefficients of 0.44 and 0.54, respectively. The positive correlation indicates that the $(\text{BChl-}c)_n$ with the longer-wavelength fluorescence bands transfers the excitation energy to the baseplate more efficiently. The correlation can be interpreted qualitatively by assuming the Förster mechanism of ET from $(\text{BChl-}c)_n$ to

BChl-*a*, although this interpretation has not yet been corroborated completely (40,41). According to the Förster-type ET mechanism, the (BChl-*c*)$_n$ with fluorescence bands at longer wavelengths has larger spectral overlaps with the baseplate BChl-*a*'s, which have an almost invariant spectrum. Fig. 4 *C* also shows the linear correlation of the fluorescence peak wavelength of (BChl-*c*)$_n$ with that of BChl-*a* with a slope of 0.37. The slope of <1 suggests a lower diversity in the fluorescence peak wavelength of BChl-*a*. The image in Fig. 4 *C* seems to represent the larger spectral overlap between the longer-wavelength (BChl-*c*)$_n$ and the baseplate BChl-*a*.

A clear positive correlation was observed between the asymmetry parameter *b* and $\lambda_{BCh\text{-}c}$ for the floating *Cfl.* chlorosomes with a correlation coefficient of 0.74, indicating that the (BChl-*c*)$_n$ fluorescence spectra at longer wavelengths are more symmetric. At a cryogenic temperature, the HFP and the intra-IDF mainly affect the shape of the fluorescence spectrum of a single chlorosome. The HFP in this case is not determined by the lifetime of the excited state because the widths of the fluorescence spectra of single chlorosomes are much wider than those expected from the inverse of the excited-state lifetime. The phonon-sideband shape probably affects the HFP. Further experimental and theoretical studies are required to understand the origin of the correlation observed in Fig. 4 *B*.

CONCLUDING REMARKS

We measured fluorescence spectra of single chlorosomes at cryogenic temperature to obtain new insights into the excited state of chlorosome. Single chlorosomes of *Cfl.* and *Cb.* showed different fluorescence spectra. The spectral widths were much broader for single *Cfl.* chlorosomes than for single *Cb.* chlorosomes. The former showed fluorescence spectra with single peaks, whereas the latter showed spectra with multiple peaks. The above difference, first detected in this study, suggests different diversities in the structure of the chlorosomes between the two species. The detection of single-chlorosome fluorescence enabled us to evaluate various quantities. In *Cfl.* chlorosomes, a linear correlation was found between the $F_{BChl\text{-}a}/F_{BChl\text{-}c}$ ratio and the peak-wavelength $\lambda_{BChl\text{-}c}$ of (BChl-*c*)$_n$ fluorescence. This finding can be qualitatively accounted for by assuming the Förster-type ET between (BChl-*c*)$_n$ and BChl-*a* in chlorosomes.

By comparing the $\lambda_{BChl\text{-}c}$ distribution to the IDF determined by the hole-burning studies, the extent of inhomogeneity within a single chlorosome was estimated. *Cb.* chlorosomes were shown already inhomogeneously broadened at the single-chlorosome level. In the single *Cfl.* chlorosomes, on the other hand, it was shown that the inhomogeneous broadening within a single chlorosome provides only a minor contribution to the broadening of the fluorescence profiles.

This work was supported in part by Grants-in-Aid for Scientific Research (15370067, 17370055, 15350107, 17029065, and 17750010), the 21st COE program for ''the origin of the universe and matter'' from the Japanese Ministry of Education, Science, Sports, and Culture, and the Japan Society for the Promotion of Science. The work was also supported by the Academic Frontier Project for Private Universities, matching fund subsidy from the Japanese Ministry of Education, Science, Sports, and Culture, 2003-2007. Y.S. is grateful for a Japan Society for the Promotion of Science Research Fellowship for Young Scientists.

REFERENCES

1. Olson, J. M. 1980. Chlorophyll organization in green photosynthetic bacteria. *Biochim. Biophys. Acta.* 594:33–51.
2. Blankenship, R. E., J. M. Olson, and M. Miller. 1995. Antenna complexes from green photosynthetic bacteria. *In* Anoxygenic Photosynthetic Bacteria. R. E. Blankenship, M. T. Madigan, and C. E. Bauer, editors. Kluwer, Dordrecht, The Netherlands. 399–435.
3. Staehelin, L. A., J. R. Golecki, R. C. Fuller, and G. Drews. 1978. Visualization of supramolecular architecture of chlorosomes (*Chlorobium*-type vesicles) in freeze-fractured cells of *Chloroflexus aurantiacus*. *Arch. Microbiol.* 119:269–277.
4. Staehelin, L. A., J. R. Golecki, and G. Drews. 1980. Supramolecular organization of chlorosomes (chlorobium vesicles) and of their membrane attachment sites in *Chlorobium limicola*. *Biochim. Biophys. Acta.* 589:30–45.
5. Tamiaki, H. 1996. Supramolecular structure in extramembraneous antennae of green photosynthetic bacteria. *Coord. Chem. Rev.* 148: 183–197.
6. Olson, J. M. 1998. Chlorophyll organization and function in green photosynthetic bacteria. *Photochem. Photobiol.* 67:61–75.
7. Frigaard, N.-U., A. G. M. Chew, H. Li, J. A. Maresca, and D. A. Bryant. 2003. *Chlorobium tepidum*: insights into the structure, physiology, and metabolism of a green sulfur bacterium derived from the complete genome sequence. *Photosynth. Res.* 78:93–117.
8. Balaban, T. S., H. Tamiaki, and A. R. Holzwarth. 2005. Chlorins programmed for self-assembly. *In* Supramolecular Dye Chemistry. Topics in Current Chemistry series, Vol. 258. F. Würthner, editor. Springer, Heidelberg, Germany. 1–38.
9. Frigaard, N.-U., S. Takaichi, M. Hirota, K. Shimada, and K. Matsuura. 1997. Quinones in chlorosomes of green sulfur bacteria and their role in the redox-dependent fluorescence studied in chlorosome-like bacteriochlorophyll *c* aggregates. *Arch. Microbiol.* 167:343–349.
10. Frigaard, N.-U., K. Matsuura, M. Hirota, M. Miller, and R. P. Cox. 1998. Studies of the location and function of isoprenoid quinones in chlorosomes from green sulfur bacteria. *Photosynth. Res.* 58:81–90.
11. Holzwarth, A. R., and K. Schaffner. 1994. On the structure of bacteriochlorophyll molecular aggregates in the chlorosomes of green bacteria. A molecular modelling study. *Photosynth. Res.* 41:225–233.
12. Steensgaard, D. B., H. Wackerbarth, P. Hildebrandt, and A. R. Holzwarth. 2000. Diastereoselective control of bacteriochlorophyll *e* aggregation. 3^1S-BChl-*e* is essential for the formation of chlorosome-like aggregates. *J. Phys. Chem. B.* 104:10379–10386.
13. Prokhorenko, V. I., D. B. Steensgaard, and A. R. Holzwarth. 2000. Exciton dynamics in the chlorosomal antennae of the green bacteria *Chloroflexus aurantiacus* and *Chlorobium tepidum*. *Biophys. J.* 79: 2105–2120.
14. Pšenčík, J., T. P. Ikonen, P. Laurinmäki, M. C. Merckel, S. J. Butcher, R. E. Serimaa, and R. Tuma. 2004. Lamellar organization of pigments in chlorosomes, the light harvesting complexes of green photosynthetic bacteria. *Biophys. J.* 87:1165–1172.
15. Balaban, T. S. 2005. Tailoring porphyrins and chlorins for self-assembly in biomimetic artificial antenna systems. *Acc. Chem. Res.* 38: 612–623.

16. Miyatake, T., and H. Tamiaki. 2005. Self-aggregates of bacteriochlorophylls-*c, d* and *e* in a light-harvesting antenna system of green photosynthetic bacteria: Effect of stereochemistry at the chiral 3-(1-hydroxyethyl) group on the supramolecular arrangement of chlorophyllous pigments. *J. Photochem. Photobiol. C: Photochem. Rev.* 6:89–107.

17. Balaban, T. S., A. R. Holzwarth, K. Schaffner, G. J. Boender, and H. J. M. de Groot. 1995. CP-MAS ^{13}C-NMR dipolar correlation spectroscopy of ^{13}C enriched chlorosomes and isolated bacteriochlorophyll *c* aggregates of *Chlorobium tepidum*: the self-organization of pigments is the main structural feature of chlorosomes. *Biochemistry.* 34:15259–15266.

18. Mizoguchi, T., S. Sakamoto, Y. Koyama, K. Ogura, and F. Inagaki. 1998. The structure of the aggregate form of bacteriochlorophyll *c* showing the Q_y absorption above 740 nm as determined by the ring-current effects on 1H and 13C nuclei and by 1H–1H intermolecular NOE correlations. *Photochem. Photobiol.* 67:239–248.

19. van Rossum, B.-J., G. J. Boender, F. M. Mulder, J. Raap, T. S. Balaban, A. Holzwarth, K. Schaffner, S. Prytulla, H. Oschkinat, and H. J. M. de Groot. 1998. Multidimensional CP-MAS ^{13}C NMR of uniformly enriched chlorophyll. *Spectrochim. Acta [A].* 54:1167–1176.

20. van Rossum, B.-J., D. B. Steensgaard, F. M. Mulder, G. J. Boender, K. Schaffner, A. R. Holzwarth, and H. J. M. de Groot. 2001. A refined model of the chlorosomal antenna of the green bacterium chlorobium *tepidum* from proton chemical shift constraints obtained with high-field 2-D and 3-D MAS NMR dipolar correlation spectroscopy. *Biochemistry.* 40:1587–1595.

21. Prokhorenko, V. I., D. B. Steensgaard, and A. R. Holzwarth. 2003. Exciton theory for supramolecular chlorosomal aggregates: 1. Aggregate size dependence of the linear spectra. *Biophys. J.* 85:3173–3186.

22. Saga, Y., T. Wazawa, T. Nakada, Y. Ishii, T. Yanagida, and H. Tamiaki. 2002. Fluorescence emission spectroscopy of single light-harvesting complex from green filamentous photosynthetic bacteria. *J. Phys. Chem. B.* 106:1430–1433.

23. Saga, Y., T. Wazawa, T. Mizoguchi, Y. Ishii, T. Yanagida, and H. Tamiaki. 2002. Spectral heterogeneity in single light-harvesting chlorosomes from green sulfur photosynthetic bacterium *Chlorobium tepidum*. *Photochem. Photobiol.* 75:433–436.

24. Saga, Y., T. Wazawa, Y. Ishii, T. Yanagida, and H. Tamiaki. 2006. Single supramolecule spectroscopy of natural and alkaline-treated chlorosomes from green sulfur photosynthetic bacteria. *J. Nanosci. Nanotech.* 6:1750–1757.

25. Saga, Y., H. Tamiaki, Y. Shibata, and S. Itoh. 2005. Excitation energy transfer in individual light-harvesting chlorosome from green photosynthetic bacterium *Chloroflexus aurantiacus* at cryogenic temperature. *Chem. Phys. Lett.* 409:34–37.

26. Saga, Y., and H. Tamiaki. 2004. Fluorescence spectroscopy of single photosynthetic light-harvesting supramolecular systems. *Cell Biochem. Biophys.* 40:149–165.

27. van Oijen, A. M., M. Ketelaars, J. Köhler, T. J. Aartsma, and J. Schmidt. 1999. Unraveling the electronic structure of individual photosynthetic pigment-protein complexes. *Science.* 285:400–402.

28. Sprague, S. G., and A. R. Varga. 1986. Photosynthetic membranes and light harvesting systems. *In* Encyclopedia of Plant Physiology, Vol. 19. L. A. Staehelin and C. J. Arntzen, editors. Springer-Verlag, Berlin, Germany. 603–619.

29. Gerola, P. D., and J. M. Olson. 1986. A new bacteriochlorophyll a-protein complex associated with chlorosomes of green sulfur bacteria. *Biochim. Biophys. Acta.* 848:69–76.

30. Sevilla, J. M., M. Dominguez, F. Garcia-Blanco, and M. Blazquez. 1989. Resolution of absorption spectra. *Comput. Chem.* 13:197–200.

31. Hoff, W. D., I. H. M. van Stokkum, H. J. van Ramesdonk, M. E. van Brederode, A. M. Brouwer, J. C. Fitch, T. E. Meyer, R. van Grondelle, and K. J. Hellingwerf. 1994. Measurement and global analysis of the absorbance changes in the photocycle of the photoactive yellow protein from *Ectothiorhodospira halophila*. *Biophys. J.* 67:1691–1705.

32. He, J.-A., L. Samuelson, L. L. Kumar, and S. K. Tripathy. 1998. Photoelectric properties of oriented bacteriorhodopsin/polycation multilayers by electrostatic layer-by-layer assembly. *J. Phys. Chem. B.* 102:7067–7072.

33. Pšenčík, J., T. Polívka, P. Němec, J. Dian, J. Kudrna, P. Malý, and J. Hála. 1998. Fast energy transfer and exciton dynamics in chlorosomes of the green sulfur bacterium *Chlorobium tepidum*. *J. Phys. Chem.* 102:4392–4398.

34. Granzhan, A., A. Penzkofer, and G. Hauska. 2004. Photo-degradation of bacteriochlorophyll c in intact cells and extracts from Chlorobium *tepidum*. *J. Photochem. Photobiol. A: Chem.* 165:75–89.

35. Mimuro, M., M. Hirota, Y. Nishimura, T. Moriyama, I. Yamazaki, K. Shimada, and K. Matsuura. 1994. Molecular organization of bacteriochlorophyll in chlorosomes of the green photosynthetic bacterium *Chloroflexus aurantiacus*: studies of fluorescence depolarization accompanied by energy transfer processes. *Photosynth. Res.* 41:181–191.

36. Mauring, K., V. Novoderezhkin, A. Taisova, and Z. G. Fetisova. 1999. Exciton levels structure of antenna bacteriochlorophyll *c* aggregates in the green bacterium *Chloroflexus aurantiacus* as probed by 1.8–293 K fluorescence spectroscopy. *FEBS Lett.* 456:239–242.

37. Fetisova, Z. G., and K. Mauring. 1992. Experimental evidence of oligomeric organization of antenna bacteriochlorophyll *c* aggregates in the green bacterium *Chloroflexus aurantiacus* by spectral hole burning. *FEBS Lett.* 307:371–374.

38. Borrego, C. M., P. D. Gerola, M. Miller, and R. P. Cox. 1999. Light intensity effects on pigment composition and organization in the green sulfur bacterium *Chlorobium tepidum*. *Photosynth. Res.* 59:159–166.

39. Tamiaki, H. 2005. Self-aggregates of natural and modified chlorophylls as photosynthetic light-harvesting antenna systems: substituent effect on the B-ring. *Photochem. Photobiol. Sci.* 4:675–680.

40. Causgrove, T. P., D. C. Brune, and R. E. Blankenship. 1992. Förster energy transfer in chlorosomes of green photosynthetic bacteria. *J. Photochem. Photobiol. B: Biol.* 15:171–179.

41. Fetisova, Z., A. Freiberg, K. Mauring, V. Novoderezhkin, A. Taisova, and K. Timpmann. 1996. Excitation energy transfer in chlorosomes of green bacteria: theoretical and experimental studies. *Biophys. J.* 71: 995–1010.